SEPARATION OF THREE-COMPONENT GAS MIXTURE BY MEANS OF A MICROPOROUS GLASS MEMBRANE WITH COCURRENT FLOW

YUJI SHINDO, TOSHIKATSU HAKUTA, HIROSHI YOSHITOME AND HAKUAI INOUE

Process Research and Development Division, National Chemical Laboratory for Industry, Tsukuba, Ibaraki 305

Key Words: Membrane Separation, Porous Membrane, Microporous Glass, Cocurrent Flow, Perfect Mixing, Multicomponent Gas Separation, Gas Diffusion, Gas Permeation

To investigate the separation of a multicomponent mixture by means of a microporous glass membrane, experiments in the separation of a ternary mixture composed of helium, oxygen and argon were performed with cocurrent flow operation at 407 K. The pressure of the feed stream was 175 kPa and 216 kPa, while the pressure of the permeate stream was maintained at atmospheric. The cut was made to vary by changes in feed-gas flow rate. Theoretical analysis was made on the basis of some assumptions. The agreement between theoretical values and experimental data for both permeated and rejected gas composition was fairly good. In addition, the effect of longitudinal mixing in both feed and permeate streams, and the usefulness and limitations of the model, were studied.

Introduction

A number of studies[2,4,5,9,10] of gas separation by means of a microporous glass membrane have been reported. Microporous glass membranes have great advantages in chemical and thermal stabilities[12,14,15] as well as high permeability. Kameyama *et al.*[7,8] have demonstrated selective permeation and concentration of hydrogen produced by the decomposition of hydrogen sulfide by means of a microporous glass membrane at high temperatures. In a similar manner, Shinji *et al.*[16] separated hydrogen from a gas mixture of cyclohexane, benzene and hydrogen. In membrane applications to an actual gas separation system, we often encounter the problem of predicting the performance of a multicomponent system. There are, however, few reports regarding multicomponent gas separation by means of a microporous glass membrane.

In this study, gas separation by permeation through a microporous glass membrane for a ternary system with cocurrent flow was performed. Experimental data were compared with theoretical values on the basis of some assumptions. Also, the influence of gaseous mixing along the membrane on the separation and the availability and limitations of the assumptions are discussed.

Received November 26, 1984. Correspondence concerning this article should be addressed to Y. Shindo. H. Inoue is at Dept. of Chem. Eng., Univ. of Tokyo, Tokyo 113.

1. Experimental

1.1 Experimental apparatus

The experimental apparatus was the same as described earlier.[15] Cylindrical microporous glass was used as a permeable membrane. The physical properties of the microporous glass membrane are indicated in **Table 1**.

1.2 Pore diameter and gas permeability of microporous glass

The pore-size distribution of the microporous glass was measured by nitrogen desorption. It had a narrow pore-size distribution and a mean pore diameter of 4.0 nm, as shown in **Fig. 1**. Permeabilities of gases through the microporous glass membrane were measured. The pressure of the permeate stream was fixed at atmospheric pressure, and the pressure of the feed stream was made to vary from 120 kPa to 220 kPa in order to obtain various pressure drops across the membrane. Still, the observed permeability was pretty much constant, as shown in **Fig. 2**. The gas permeabilities are indicated in **Table 2**. The permeabilities are approximately proportional to the inverse of the square root of their molecular weight according to Knudsen's law.[11,17]

1.3 Experimental procedures

The separations were performed at 407 K. The feed stream pressure was 175 kPa and 216 kPa, while the permeate stream pressure was fixed at atmospheric pressure. The flow rate of the outlet stream was measured by a soap-film flowmeter. Analysis of the

Table 1. Physical properties of microporous glass membrane

Membrane area	151×10^{-4} m^2
Thickness	1.4 mm
Outside diameter	19 mm
Void fraction	0.28
Mean pore diameter	4.0 nm

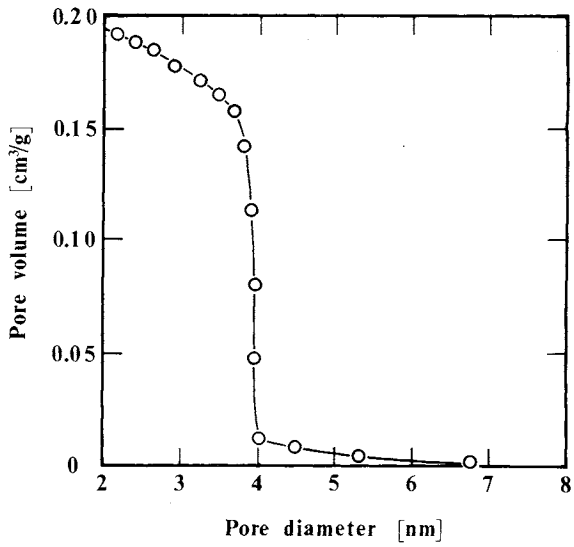

Fig. 1. Pore-size distribution of microporous glass by nitrogen desorption.

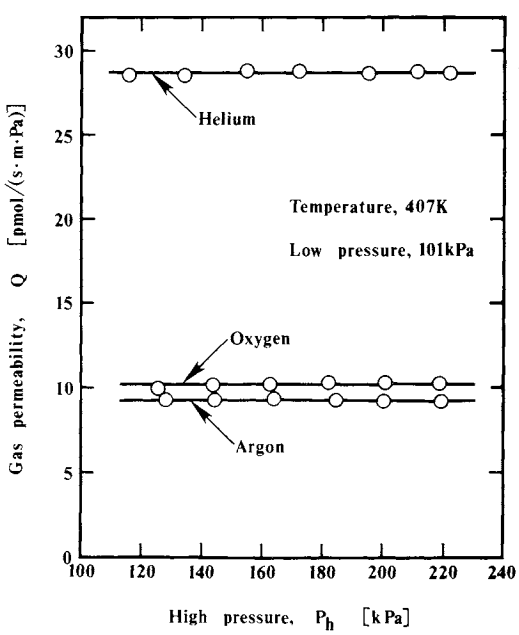

Fig. 2. Pressure effect on the gas permeability of microporous glass.

Table 2. Gas permeabilities and feed composition

	Permeability at 407 K [pmol/(s·m·Pa)]	Feed composition [−]
Helium	28.5	0.397
Oxygen	10.1	0.304
Argon	9.20	0.299

gas composition was performed by gas chromatography. The feed-gas flow rate was obtained as the sum of the reject and permeate flow rates. The feed-gas flow rate was made to vary in order to obtain various cuts.

1.4 Experimental results

The separation experiments were made with a gas mixture of helium, oxygen and argon. The feed gas composition is indicated in Table 2. The experimental results are shown in **Figs. 3** and **4**. The mole fractions of helium, oxygen and argon on both the permeated and the rejected streams, and the stage cut, are plotted against the feed-gas flow rate.

2. Analysis

2.1 Assumptions

As shown in Fig. 1, microporous glass contains no macropores, and the mean pore diameter is so small that gas molecules do not collide with each other, but only with the wall. Therefore, it may be assumed that there is no interaction between the permeating components. In the present experiments, the concentration polarization[6] is almost absent since gaseous diffusion in the streams is much larger than gaseous permeation through the membrane. The pressure loss[1,13,18] along the membrane in the permeation cell is considered negligibly small in view of the relatively low flow rates encountered in the permeation cell. Then the following assumptions were made.

(i) Permeability of each gas component is the same as that of the pure gas, and is independent of pressure.

(ii) Concentration gradients in the permeation direction are negligibly small.

(iii) Pressure drops of the feed and permeate gas streams are negligibly small.

(iv) Plug flow exists in the feed and permeate streams.

2.2 Cocurrent flow

The experimental results were compared with the theoretical values on the basis of the assumptions described above. The permeation cell is separated into two sections by a microporous glass membrane. **Figure 5** is a schematic diagram of the permeation cell in cocurrent flow. Taking total and component balances over the differential area dA, one can obtain the following system of differential equations.

$$-dF = dG \tag{1}$$

$$= dA \sum_{k=1}^{n} Q_k (P_h x_k - P_l y_k)/\delta \tag{2}$$

$$-d(x_i F) = d(y_i G) \tag{3}$$

$$= dA Q_i (P_h x_i - P_l y_i)/\delta \tag{4}$$

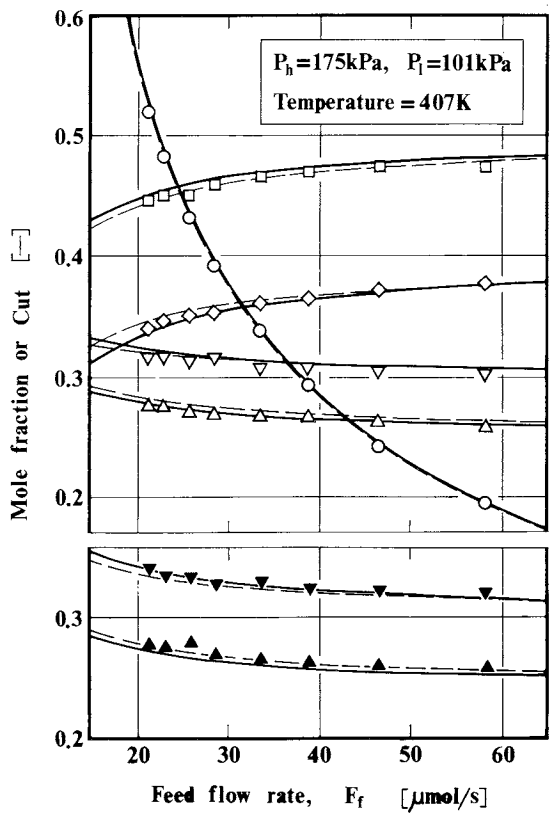

Fig. 3. Separation of helium, oxygen and argon by a microporous glass membrane. □, permeated He; ◇, rejected He; △, permeated O_2; ▽, rejected O_2; ▲, permeated Ar; ▼, rejected Ar; ○, cut; ——, theoretical cocurrent flow; – – – –, theoretical perfect mixing.

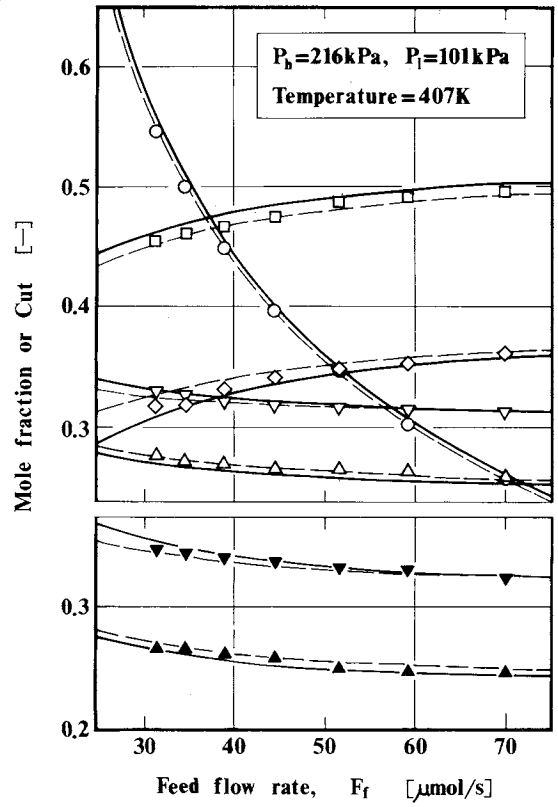

Fig. 4. Separation of helium, oxygen and argon by a microporous glass membrane. □, permeated He; ◇, rejected He; △, permeated O_2; ▽, rejected O_2; ▲, permeated Ar; ▼, rejected Ar; ○, cut; ——, theoretical cocurrent flow; – – – –, theoretical perfect mixing.

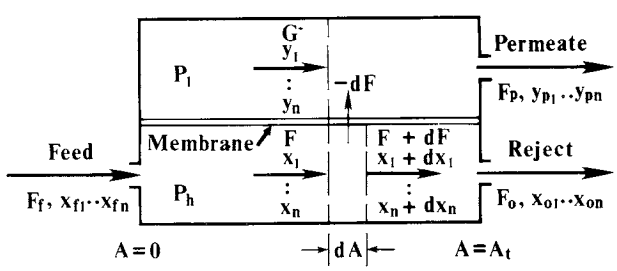

Fig. 5. Schematic diagram of cocurrent permeation cell.

$$\sum_{k=1}^{n} x_k = 1 \tag{5}$$

$$\sum_{k=1}^{n} y_k = 1 \tag{6}$$

where F is the flow rate of the feed (high-pressure) stream; G is the flow rate of the permeate (low-pressure) stream; n is the number of components; Q_i is the permeability of component i; P_h and P_l are the pressures on the feed side and the permeate side, respectively; x_i and y_i are the mole fractions of component i on the feed side and the permeate side, respectively; and δ is the membrane thickness.

Integration of Eqs. (1) and (3) from the inlet point to an arbitrary point yields

$$G = F_f - F \tag{7}$$

$$y_i = \frac{x_{fi}F_f - x_i F}{F_f - F}, \qquad A \neq 0 \quad (i = 1, \cdots, n-1) \tag{8}$$

where F_f is the feed flow rate at the inlet; x_{fi} is the mole fraction of component i. At $A=0$, the mole fraction y_{fi} is obtained by a limiting process of the l'Hospital rule as $F \to F_f$.

$$y_{fi} = \frac{Q_i(P_h x_{fi} - P_l y_{fi})}{\sum_{k=1}^{n} Q_k(P_h x_{fk} - P_l y_{fk})}, \qquad A = 0 \tag{9}$$

Equation (9) implies that over the first incremental section the cell behaves as in perfect mixing. The mole fractions on the permeate side at $A=0$ can be obtained by solving the simultaneous equations, Eq. (9) for all components. On dividing Eq. (9) by the member of Eq. (9) for component j, one obtains

$$\frac{y_{fi}}{y_{fj}} = \frac{Q_i(P_h x_{fi} - P_l y_{fi})}{Q_j(P_h x_{fj} - P_l y_{fj})} \tag{10}$$

Solving for y_{fj} yields

$$y_{fj} = \frac{x_{fj} Q_j / Q_i}{P_l/P_h\{(Q_j/Q_i) - 1\} + (x_{fi}/y_{fi})} \qquad (j \neq i, n) \tag{11}$$

Substituting Eq. (11) into Eq. (6) gives

$$\sum_{k=1}^{n} \frac{x_k Q_k/Q_i}{P_l/P_h\{(Q_k/Q_i)-1\}+(x_{fi}/y_{fi})}=1, \qquad A=0 \quad (12)$$

Solution of Eq. (12) gives the value of the mole fraction of component i in the permeate stream at $A=0$. The mole fractions of the other components at $A=0$ are calculated by the aid of Eqs. (11) and (6). Rearrangement of Eq. (2) yields

$$\frac{dF}{dA}=-\sum_{k=1}^{n} Q_k(P_h x_k-P_l y_k)/\delta \quad (13)$$

Substitution of dF from Eq. (2) into Eq. (4), followed by rearrangement, gives

$$\frac{dx_i}{dA}=-\left\{Q_i(P_h x_i-P_l y_i)/\delta-x_i\sum_{k=1}^{n} Q_k(P_h x_k-P_l y_k)/\delta\right\}\Big/F \quad (i=1,\cdots,n-1) \quad (14)$$

The value of x_n is obtained by Eq. (5). The stage cut θ is defined as

$$\theta=\frac{F_p}{F_f} \quad (15)$$

where F_p is the flow rate of the permeate stream at the outlet.

The theoretical values of the mole fractions at the outlet, x_{oi}'s and y_{pi}'s, and the cut θ are obtained by integration of the system differential equations, Eqs. (13) and (14), in conjunction with Eqs. (5) to (8), and Eqs. (11) and (12). The calculation procedure is as follows.

(1) At $A=0$, the value of y_{fi} is obtained by solving Eq. (12). Then, the values of y_{fj}'s ($j\neq i, n$) are calculated by use of Eq. (11), and the value of y_{fn} is obtained by the relation of Eq. (6).

(2) From $A=0$ to $A=A_t$, integration of Eqs. (13) and (14) are carried out with initial conditions

$$F=F_f, \quad x_i=x_{fi}, \quad y_i=y_{fi} \quad (i=1,\cdots,n) \quad \text{at} \quad A=0 \quad (16)$$

The values of G and y_i's at each point are calculated by Eqs. (7), (8) and (6).

(3) At $A=A_t$, the values of x_{oi}'s, y_{pi}'s and F_p are derived, then the cut θ is calculated by Eq. (15).

The theoretical values on the basis of cocurrent flow are shown in Figs. 3 and 4 by solid lines. It can be seen from Figs. 3 and 4 that the theoretical values agree well with the experimental data.

3. Discussion

3.1 Effect of longitudinal mixing

The theoretical values were derived on the basis that there was plug flow on both sides of the membrane. It is, of course, improbable that such conditions actually exist. Longitudinal mixing[3] in both the feed and the permeate streams may occur to some extent. The extreme situation of mixing is perfect mixing. The experimental data were compared with the theoretical values on the basis of perfect mixing. The theoretical values were calculated as shown below.

Figure 6 shows permeation for the perfect mixing case. Mass conservation yields

$$x_{fi}=(1-\theta)x_{oi}+\theta y_{pi} \quad (i=1,\cdots,n) \quad (17)$$

Taking component balance on the permeate side one obtains

$$y_{pi}F_p=A_t Q_i(P_h x_{oi}-P_l y_{pi})/\delta \quad (18)$$

On dividing Eq. (18) by the member of Eq. (18) with $i=j$, one obtains

$$\frac{y_{pi}}{y_{pj}}=\frac{Q_i(P_h x_{oi}-P_l y_{pi})}{Q_j(P_h x_{oj}-P_l y_{pj})} \quad (19)$$

Eliminating x_{oi} and x_{oj} by the aid of Eq. (17) and solving for y_{pj} yields

$$y_{pj}=\frac{x_{fj}Q_j/Q_i}{(\gamma+\theta-\gamma\theta)\{(Q_j/Q_i)-1\}+(x_{fi}/y_{pi})} \quad (j\neq i, n) \quad (20)$$

where γ is the pressure ratio, defined as

$$\gamma=\frac{P_l}{P_h} \quad (21)$$

On substituting Eq. (20) into Eq. (6), we obtain

$$\sum_{k=1}^{n} \frac{x_{fk}Q_k/Q_i}{(\gamma+\theta-\gamma\theta)\{(Q_k/Q_i)-1\}+(x_{fi}/y_{pi})}=1 \quad (22)$$

The solution of Eq. (22) gives the theoretical value of y_{pi}. The material balance over the overall membrane surface area leads to

$$\theta F_f=A_t\sum_{k=1}^{n} Q_k(P_h x_{ok}-P_l y_{pk})/\delta \quad (23)$$

The solution procedure for perfect mixing is to make a guess of the value of θ, then calculate y_{pi}'s and x_{oi}'s ($i=1,\cdots,n$) by Eqs. (22), (20), (6) and (17), and check if y_{pi}'s and x_{oi}'s satisfy Eq. (23). If not, a new guess must be made and the procedure repeated till Eq. (23) is satisfied.

The theoretical values with the assumption of perfect mixing are shown in Figs. 3 and 4 with dashed lines. There is little difference between the theoretical values for the cocurrent and perfect mixing cases. It may be said that the effect of longitudinal mixing is very small in the present experiments.

It is found that the difference between the theoretical values for cocurrent flow and perfect mixing in Fig. 4 is larger than that in Fig. 3. This caused by the difference in operating pressures. It is noted that the magnitude of the difference between the flow patterns

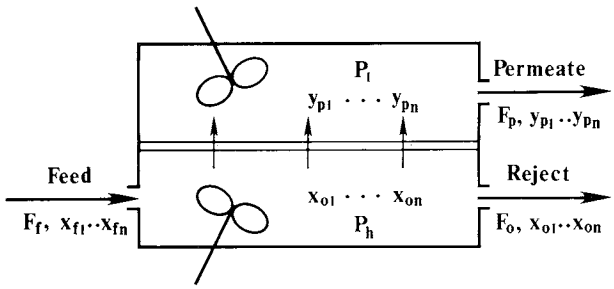

Fig. 6. Schematic diagram of perfect-mixing permeation cell.

depends on the operating conditions: feed composition, operation pressure, stage cut, etc.

3.2 Usefulness and limitations of the model

Under given operational conditions, the validity of assumption (i) depends on the nature of the gas-membrane system, while the validity of assumptions (ii)–(iv) depends on the cell geometry. Assumption (i) may also be valid for nonporous polymetric membranes of very dilute systems and the mixed permeation of gases with low critical temperatures, such as the permanent gases.

Conclusion

Separations of ternary gas mixture by permeation through a microporous glass membrane with cocurrent flow were performed. Theoretical values were calculated on the basis of some assumptions. There was good agreement between experimental and theoretical values. The effect of longitudinal mixing in both feed and permeate streams was studied. In the present experiments, the mixing effect on the separation was very small. The calculation method presented in this paper is applicable to prediction of multicomponent gas separation by permeation through microporous glass and other permeation systems where the pure gas theory (assumption (i)) is valid.

Nomenclature

A	=	membrane area	[m²]
A_t	=	total membrane area	[m²]
F	=	flow rate of feed stream	[mol/s]
F_f	=	flow rate of feed stream at inlet	[mol/s]
F_o	=	flow rate of feed stream at outlet	[mol/s]
F_p	=	flow rate of permeate stream at outlet	[mol/s]
G	=	flow rate of permeate stream	[mol/s]
n	=	number of components	[—]
P_h	=	pressure of feed stream	[Pa]
P_l	=	pressure of permeate stream	[Pa]
Q	=	gas permeability	[pmol/(s·m·Pa)]
x	=	mole fraction of gas component in feed stream	[—]
x_f	=	mole fraction of gas component in feed stream at inlet	[—]
x_0	=	mole fraction of gas component in feed stream at outlet	[—]
y	=	mole fraction of gas component in permeate stream	[—]
y_f	=	mole fraction of gas component in permeate stream at $A=0$	[—]
y_p	=	mole fraction of gas component in permeate stream at outlet	[—]
γ	=	pressure ratio, P_l/P_h	[—]
δ	=	thickness of membrane	[m]
θ	=	stage cut, F_p/F_f	[—]

〈Subscripts〉

i, j, k	=	component indication

Literature Cited

1) Berman, A. S.: *J. Appl. Phys.*, **24**, 1232 (1953).
2) Blaisedell, C. T. and K. Kammermeyer: *Chem. Eng. Sci.*, **28**, 1249 (1973).
3) Breuer, M. E. and K. Kammermeyer: *Separ. Sci.*, **2**, 319 (1967).
4) Huckins, E. H. and K. Kammermeyer: *Chem. Eng. Prog.*, **49**, 180 (1953).
5) Huckins, E. H. and K. Kammermeyer: *Chem. Eng. Prog.*, **49**, 294 (1953).
6) Hwang, S. T. and K. Kammermeyer: "Membranes in Separations," p. 44, John Wiley & Sons, New York (1975).
7) Kameyama, T., M. Dokiya, M. Fujishige, H. Yokokawa and K. Fukuda: *Ind. Eng. Chem. Fundam.*, **20**, 97 (1981).
8) Kameyama, T., M. Dokiya, M. Fujishige, H. Yokokawa and K. Fukuda: *Int. J. Hydrogen Energy*, **8**, 5 (1983).
9) Kammermeyer, K. and D. D. Wyrick: *Ind. Eng. Chem.*, **50**, 1309 (1958).
10) Kammermeyer, K. and H. T. Ward: *Ind. Eng. Chem.*, **33**, 474 (1941).
11) Knudsen, M.: *Ann. Phys.*, **28**, 705 (1909).
12) Nordberg, M. E.: *J. Am. Ceram. Soc.*, **27**, 299 (1944).
13) Pan, C. Y. and H. W. Habgood: *Can. J. Chem. Eng.*, **56**, 210 (1978).
14) Shindo, Y., T. Hakuta, H. Yoshitome and H. Inoue: *J. Chem. Eng. Japan*, **16**, 120 (1983).
15) Shindo, Y., T. Hakuta, H. Yoshitome and H. Inoue: *J. Chem. Eng. Japan*, **17**, 650 (1984).
16) Shinji, O., M. Misonou and Y. Yoneda: Preprints for 46th Symposium on Catalysis, Japan, 4005, Sendai (1980).
17) Smoluchowski, M.: *Ann. Phys.*, **33**, 1559 (1910).
18) Thorman, M., H. Rhim and S. T. Hwang: *Chem. Eng. Sci.*, **30**, 751 (1974).